Open Archive Toulouse Archive Ouverte (OATAO)

OATAO is an open access repository that collects the work of some Toulouse researchers and makes it freely available over the web where possible.

This is an author's version published in: https://oatao.univ-toulouse.fr/26571

Official URL: https://doi.org/10.23919/EuCAP48036.2020.9135692

To cite this version :

Any correspondence concerning this service should be sent to the repository administrator: tech-oatao@listes-diff.inp-toulouse.fr

A Bird-Cage Coil for MRI Studies of Unsaturated Granular Materials

Sina Marhbaie* Hakim Takhedmit†, Patrick Poulichet‡, Marjorie Grzeskowiak§, Abdoulaye Fall*

*Laboratoire Navier (UMR 8205 CNRS, IFSTTAR, Ecole des Ponts ParisTech), Université de Paris-Est, Champs-sur-Marne, France
sina.marhabaie@u-pem.fr, abdoulaye.fall@ifsttar.fr
†Université de Paris-Est Marne-la-Valle, UPEMLV, ESYCOM, Marne-la-Vallee, France, hakim.takhedmit@u-pem.fr
‡Université de Paris-Est Marne-la-Valle, UPEMLV, ESYCOM (FRE 2028), ESIEE-Paris, CNAM, Marne-la-Vallee, France
p.poulichet@esiee.fr
§ISAE-SUPAERO, Université de Toulouse, Toulouse, France, grzeskow@univ-mlv.fr

Abstract—**Magnetic Resonance Imaging (MRI) is a powerful and non-invasive technique that can be used to reveal useful information about different types of materials. During an MRI experiment a magnetic resonance signal is induced (according to Faraday's law of induction) in a device called "probe". MRI probes are simply near field antennas designed in a specific way in order to produce a homogeneous magnetic field at a specific frequency in the region of interest. MRI is a strong technique to study unsaturated granular materials. However, it suffers from a significant drawback, that is inherent small signal-to-noise ratio. To overcome this problem the probe used for a specific MRI experiment must be optimised. In this work a bird-cage probe operating at 21.3 MHz, optimised to study unsaturated granular materials under shear stress as well as some experimental results will be presented.**

Index Terms—**Magnetic Resonance Imaging, MRI, bird-cage coil, field homogeneity mapping.**

I. INTRODUCTION

Nowadays, granular materials are almost omnipresent. They play an important role in chemical, pharmaceutical and agricultural industries as well in food and energy production [1]–[6]. In order to be able to control any industrial processes dealing with this type of materials, their specifications must be understood. In particular, the behavior of the liquid phase in wet granules is important. So far a lot of studies have been performed on saturated grain-fluid mixtures as well as dry granular materials [7]–[9], however different aspects of unsaturated granular assemblies still need to be addressed. The final aim of this work is to address microstructure of unsaturated granular materials with different liquid contents and under different flow regimes, using Magnetic Resonance Imaging (MRI).

MRI probes are the workhorses of all MRI experiments. They play an essential role in the quality of an image obtained by MRI. In clinical MRI lots of different probes with different size, shape and sensitivity exist, which enable the physician to optimise the experiment setup according to the patient's anatomy. By choosing an appropriate probe for each experiment, the physicians can obtain images with better quality within a shorter experiment time. Unsaturated granular materials contain only a few percent of liquid, that is a few percent of water, oil, or other materials that contain hydrogen atoms. Therefore, the magnetic resonance signal obtained from these materials in a typical experiment is very low. In such conditions, the same experiment has to be repeated several times in order to obtain acceptable signal-to-noise ratio (SNR). Needless to say, this requires a long experiment time. By optimising the probe to the constraints imposed on this problem, we try to increase the SNR of our experiments, so that we can obtain good images within a reasonable experiment time.

II. MRI UNDER SHEAR STRESS

In order to be able to perform an MRI experiment in a sheared unsaturated granular material, a specific holder is required. An example of such a sample holder, called shear device is shown in Fig. 1. In this device the granular materials are loaded inside the sample cell. When the top rotating cylinder starts to rotate, it exerts a shear force parallel to the surface of the rotating cylinder. This causes a shear stress to the material under study. The whole setup is then placed in an MRI scanner enabling us to perform MRI experiments on materials under shear flow in order to measure simultaneously the velocity field, the solid concentration field, the liquid distribution and the local rheology of unsaturated granular materials. The scanner used in this study was 0.5 Tesla scanner (Magnex Scientific), working at 21.3 MHz with a Bruker console. In our former setup, the shear device was placed inside a large bird-cage coil shown in Fig. 1(c). Although the B_1 homogeneity (the homogeneity of the alternating magnetic field produced by the coil) of such a setup is very good due to the fact that the sample is far away from the rungs (legs) of the coil, the low sensitivity of such a setup significantly limits its applicability to unsaturated material. Simply because the signal is too small compared to the noise level.

After a preliminary study, a bird-cage coil was opted for further improvement of our setup [10]. Fig. 2 shows our modified setup, which has been built during this work. In the modified setup, instead of placing the whole shear device inside the probe, only the sample cell is placed in the active
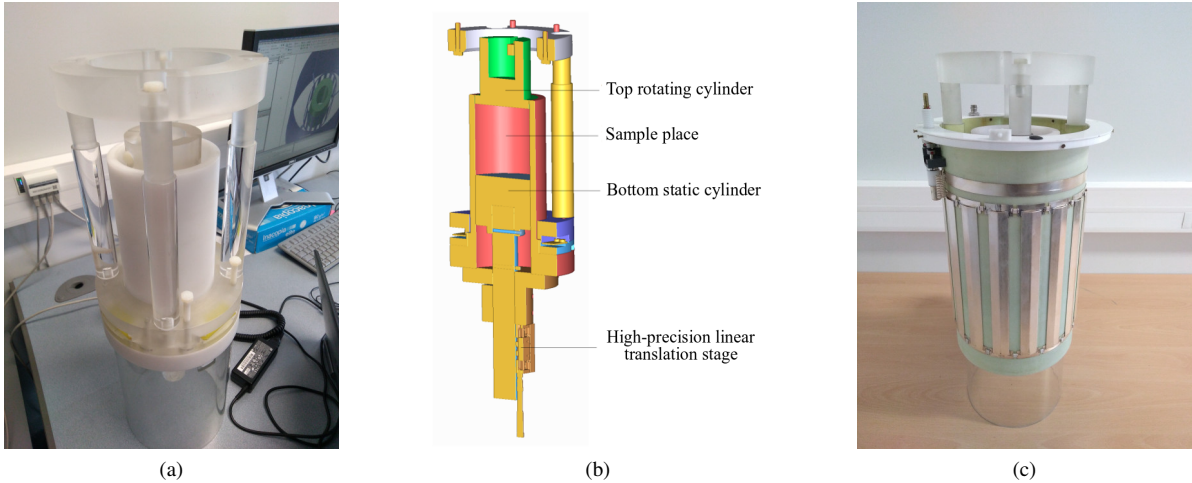
Fig. 1. (a) The device we used to hold the sample, and to apply a shear stress on the material (shear device). (b) Schematic view from the interior of the shear device. (c) Shear device inside the former bird-cage probe. In the former setup the probe was outside of the shear device, and as a result the rungs of the coil were far away from sample.

region of the probe. Since the sample is much closer to the probe in the modified setup, the sensitivity of the modified setup is expected to be higher than in the previous setup.

III. SIMULATIONS AND THEORETICAL CALCULATIONS

Bird-cage coils have been introduced long time ago. So far a lot theoretical and experimental works have been carried out on this subject. These coils can produce a homogeneous B_1 field in a large volume. Therefore, they are extensively used in clinical MRI as whole body excitation coils. They are usually modeled as a network of identical low-pass, high-pass or band-pass filters that are all coupled. Calculating the exact value of the resonance frequency of a bird-cage coil is not a straight forward task. In this work, a good estimate of the required capacitor value was obtained by using a user friendly mobile phone application "BBuilser" [11], and more accurate results was obtained by the HFSS package from ANSYS Inc. Using HFSS the dimensions of the rungs, and the capacitor values have been changed to obtain a resonance frequency around 21.3 MHz. HFSS is also able to calculate the B_1 field, and can produce a B_1 map of a coil. A typical model constructed for HFSS simulations, and a typical calculated field maps (H_1 map) are shown in Fig. 3.

IV. REALISATION OF THE PROBE

A. Coil Body Realisation

After calculating the required dimensions, a comb-shaped piece of copper were cut (out of a rectangular copper sheet with a thickness of 0.8 mm) by using a standard CNC (Computer Numerical Control) machine. By rolling this comb-shaped piece of copper the upper part of the coil were realised. The construction of the probe were completed by rolling a long copper tape (with a thickness of 0.8 mm) to form the bottom ring, and by soldering a 220 pF ceramic capacitor to each rung.

B. Realisation of the RF Shield

A piece of plastic sheet was rolled to form a cylinder which serves as a support. Then four rectangular copper sheets (with a thickness of 0.3 mm) were rolled, and glued by using a strong double sided scotch tape to the interior wall of the cylinder. Each sheet covers a quarter of the total interior surface of the cylinder. Each pair of individual sections were then bridged by soldering thirty 1nF capacitors, which are shown in yellow in Fig. 3(a). By choosing a large value for the bridging capacitors (1 nF), the shield acts like a continuous metallic cylinder at 21.3 MHz. However it performs as an open loop at low frequencies. Such a sectioned design prevents circulation of low-frequency eddy currents [12] that can be otherwise induced due to mutual coupling of the RF shield and the gradient coils of the scanner.

C. Tuning and Matching

The coil was coarse tuned by choosing an appropriate value for the rung capacitors. Fine tune is achieved by soldering a variable capacitor in parallel with the rung capacitor that is connected to the line. The position of the tune capacitor is shown in green in Fig. 3(a). The coil is matched to the line impedance by a variable capacitor soldered in series to the line. The match capacitor is depicted in violet in Fig. 3(a).

Fig. 4 depicts the reflection coefficient S_{11} of the probe. Theoretically, a bird-cage coil with 16 rungs should have 9 resonances with different frequencies [12]. For a low-pass coil the fundamental resonance mode, which is the mode that produces a homogeneous B_1 field, correspond to the resonance with the lowest frequency. By contrast, for a high pass bird-cage coil the fundamental resonance mode corresponds to the resonance with the highest frequency. Therefore, for our coil the fundamental resonance occurs around 21.3 MHz.
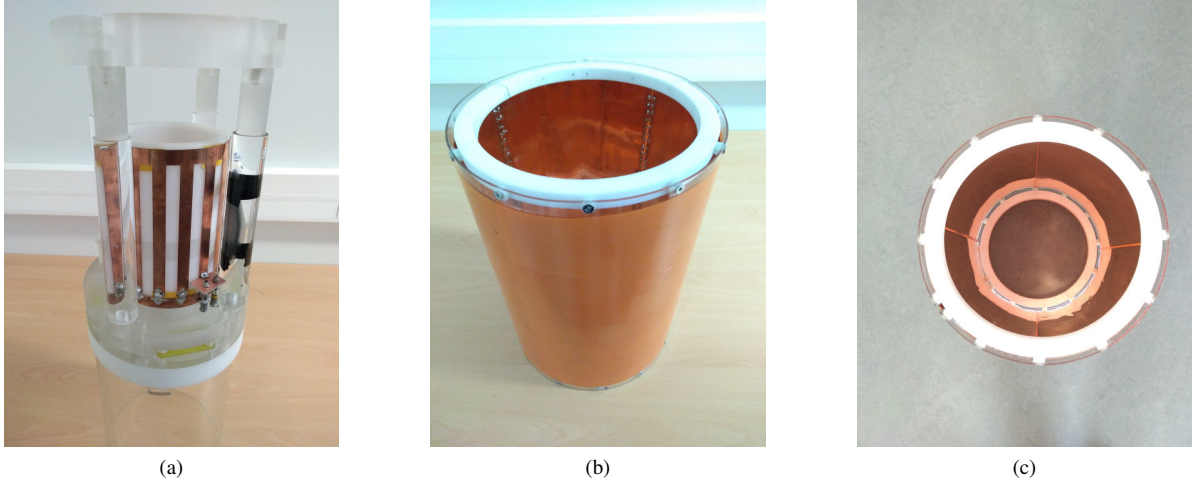
Fig. 2. (a) New probe built in this work, which has been installed right on the sample cell. The new probe is much more closer to the sample compared to the previous setup. (b) Front view of the RF shield. (c) Top view of the RF shield. In the modified setup the rungs of the coil were close to the sample and far away from the shield, and consequently the sensitivity has increased.
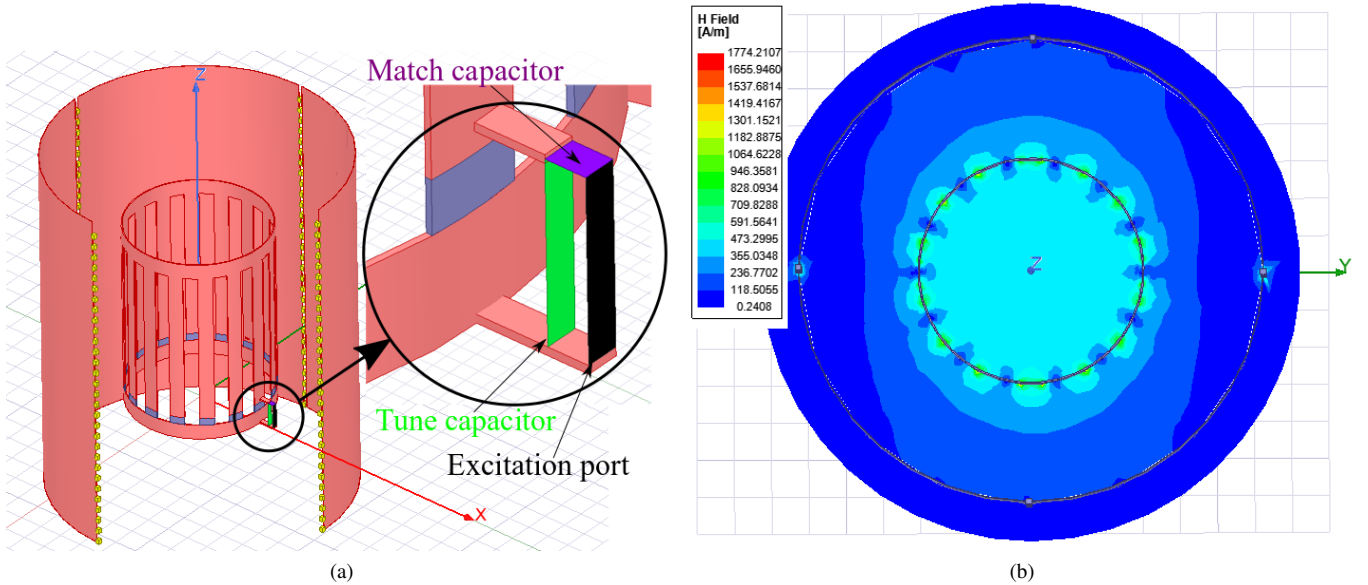

Fig. 3. (a) A typical model of our low-pass bird-cage coil used in HFSS for simulations. Those parts that were made from copper are shown in red; the rung capacitors are shown in grey, the tune capacitor is shown in green, the match capacitor is shown in violet, the excitation port is shown in black, and the bridging capacitors of the RF shield are shown in yellow. Note that only 3 sections out of the 4 sections of the RF shield are shown. (b) A typical simulated H_1 map. The circular plane is located somewhere around the center of the total height of the coil, far away from the upper and bottom rings.

V. RESULTS AND DISCUSSION

A. Nutation Curves

Fig. 5 shows the nutation curves of the previous and the modified probes. These curves were obtained by increasing the the duration of the excitation pulse in increments of 20μs, starting from 20μs. As can be seen the length of the $90°$ pulse for the modified probe is much shorter than the previous setup, 60μs for the modified probe compared to 160μs for the previous probe. This means that for the same sample the signal (measured in Watt) of the modified probe is $\left(\frac{160}{60}\right)^2 = 7.1$ times larger than the signal of the previous probe.

B. Measuring B_1 Homogeneity

For MRI applications the homogeneity of the alternating magnetic field produced by the probe, B_1, is very important. Ideally B_1 must be homogeneous in the whole region of interest. There are different techniques to measure B_1 homogeneity, among which MRI can give a high resolution map for the whole region of interest. A lot of MRI pulse sequences have been developed for this purpose [13]. MRI techniques do not directly measure B_1, but they measure the nutation angle $\theta = \gamma\tau B_1$, where γ is a constant called gyromagnetic ratio and τ is the duration of the RF pulse used for excitation. The

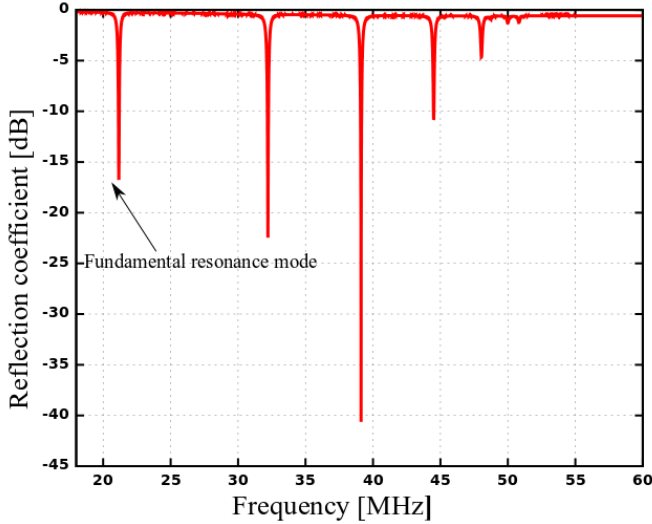Fig. 4. Reflection coefficient, S_{11}, of the tuned and matched coil. As can be seen more than one resonances exist. For a low-pass bird-cage coil, the fundamental resonance corresponds to the lowest frequency. The resonance that occur at frequencies higher than 21.3 MHz do not produce a homogeneous B_1 field.
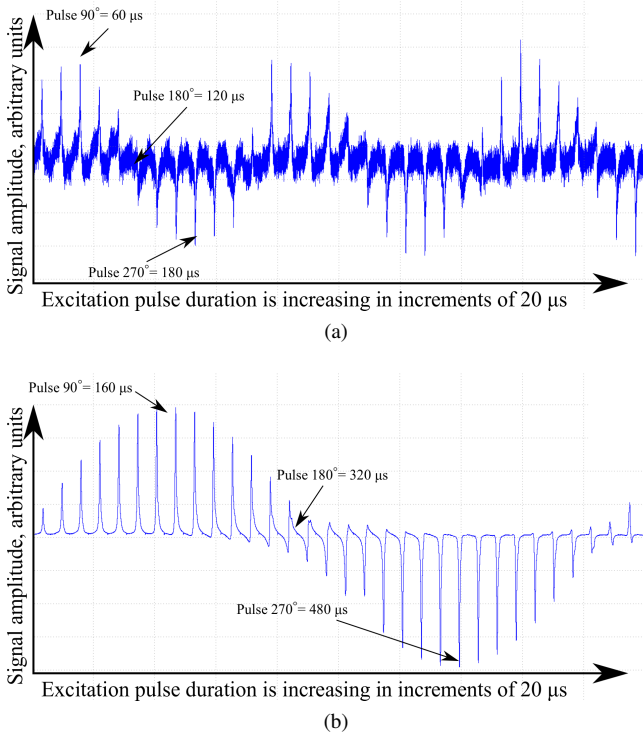

(a)

(b)

Fig. 5. Nutation curves of the new probe (a), and the previous probe (b). The length of the 90° pulse is $60\mu s$ for the new probe compared to $160\mu s$ for the previous probe. Although the noise level in (b) is much less than in (a) the setup in (a) in more sensitive for our experiment. In (b) we have more SNR simply because we have used a much larger sample. For a correct comparison the same sample has to be used for both probes.

pulse sequence we have used and the theory behind it has been described before [14]. For our experiments, this pulse sequence have been written and implemented in the Paravision program (version 4.0). The experimental data were analyzed by a home-written Python code to produce H_1 maps that are shown in Fig. 6.

In Fig. 6, the amplitude of the H_1 field, for each pixel is represented by its corresponding colour shown in the colour bar. The MRI pulse sequence we used brings about a 3D map which is represented in 8 separated 2D maps in Fig. 6. These experimental maps conform with what is expected from a bird-cage coil. That is the H_1 is more homogeneous in the central parts, and as we approach the end rings it will be perturbed. The current passing through the end rings contributes to the total H_1 field for each slice. For those slices which are far away from the end rings, this contribution is negligible, and a homogeneous H_1 field is expected. For slices which are close to the end rings, this contribution is not negligible anymore, and as a result the H_1 field is perturbed.

VI. CONCLUSION

The fabrication of a bird-cage coil optimised for MRI studies of unsaturated granular materials has been presented. The homogeneity of the produced H_1 field has been confirmed by electromagnetic simulations as well as by experimental MRI methods. This works aims toward addressing microstructure of unsaturated granular materials with different liquid contents and under different flow regimes, using MRI, which remains to be realised in future works.

ACKNOWLEDGMENT

REFERENCES

[1] N. Fraysse, H. Thomé, and L. Petit. "Humidity effects on the stability of a sandpile." The European Physical Journal B-Condensed Matter and Complex Systems 11, no. 4 (1999): 615-619.

[2] T. Mikami, K. Hidehiro, and H. Masayuki. "Numerical simulation of cohesive powder behavior in a fluidized bed." Chemical Engineering Science 53, no. 10 (1998): 1927-1940.

[3] T. C. Halsey and A. J. Levine. "How sandcastles fall." Physical Review Letters 80, no. 14 (1998): 3141.

[4] J. N. Israelachvili: Intermolecular and Surface Forces (With Applications to Colloidal and Biological Systems). Academic Press, London, 1991, 2nd ed.

[5] L. Bocquet, E. Charlaix, S. Ciliberto, and J. Crassous. "Moisture-induced ageing in granular media and the kinetics of capillary condensation." Nature 396, no. 6713 (1998): 735.

[6] D. J. Hornbaker, R. Albert, I. Albert, A.-L. Barabási, and P. Schiffer. "What keeps sandcastles standing?." Nature 387, no. 6635 (1997): 765.

[7] MiDi, G. D. R. "On dense granular flows." The European Physical Journal E. 14, no. 4 (2004): 341-365.

[8] A. Fall, G. Ovarlez, D. Hautemayou, C. Mézière, J-N. Roux, and François Chevoir. "Dry granular flows: Rheological measurements of the $\mu(I)$-rheology." Journal of rheology 59, no. 4 (2015): 1065-1080.
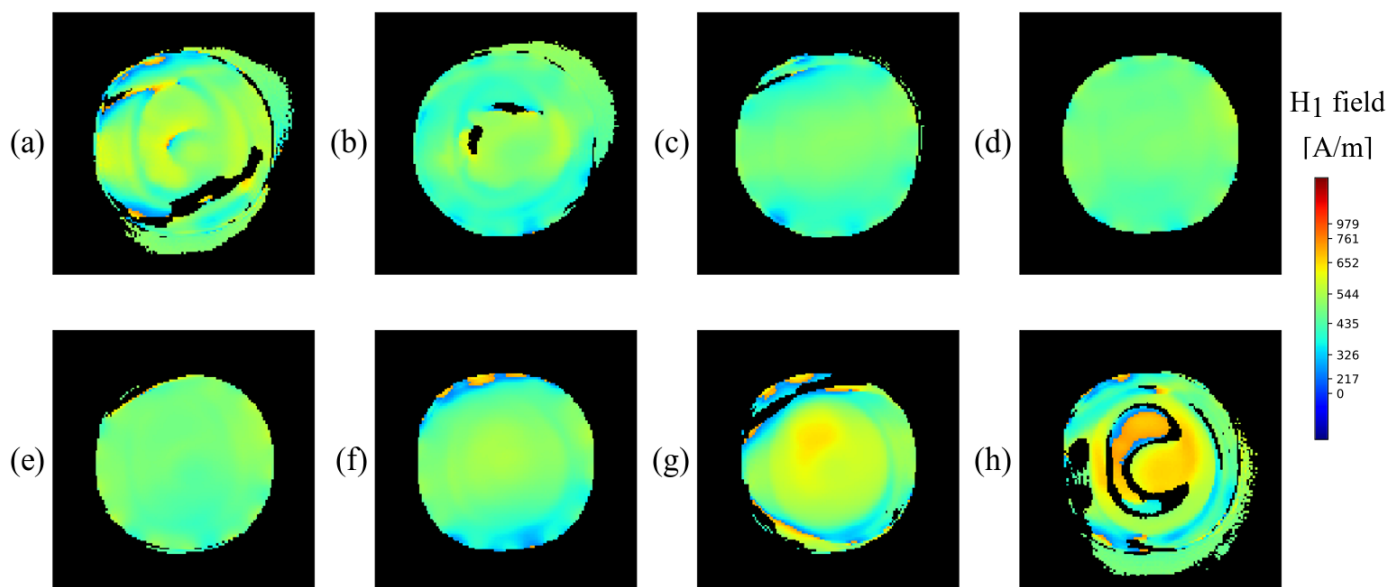
Fig. 6. Experimental H_1 maps obtained by the sequence described in [14]. The amplitude of the H_1 field, in A/m units, for each pixel is represented by the corresponding colour shown in the colour bar. The MRI experiment brings about a 3D H_1 map which is represented in 8 separated 2D maps. Each map corresponds to a 2.5 cm thick slice (in total they cover a height of 20.0 cm). From (a) to (h) the height of corresponding slice increase from a level slightly lower than the bottom ring to a level slightly higher than the upper ring.

[9] B. Andreotti, Y. Forterre, and O. Pouliquen, Granular media: between fluid and solid. Cambridge University Press, 2013.

[10] A. Waguaf, L. Fadel, V. Vigneras, F. Demontoux, A. Fall, H. Takhed-mit, and M. Grzeskowiak. "Nuclear Magnetic Resonance volumetric antenna." 13th European Conference on Antennas and Propagation (EuCAP), pp. 1-5. IEEE, 2019.

[11] C.-L. Chin, C. M. Collins, S. Li, B. J. Dardzinski, and M. B. Smith. "BirdcageBuilder: design of specified-geometry birdcage coils with desired current pattern and resonant frequency." Concepts in Magnetic Resonance: An Educational Journal 15, no. 2 (2002): 156-163.

[12] J. Mispelter, M. Lupu, and A. Briguet. "NMR probeheads for biophysical and biomedical experiments: theoretical principles & practical guide-lines.", Imperial College Press, London.

[13] R. Pohmann, and K. Scheffler, "A theoretical and experimental compar-ison of different techniques for B_1 mapping at very high fields." NMR in Biomedicine 26, no. 3 (2013): 265-275.

[14] G. R. Morrell, Morrell, Glen R. "A phase-sensitive method of flip angle mapping." Magnetic Resonance in Medicine: An Official Journal of the International Society for Magnetic Resonance in Medicine 60, no. 4 (2008): 889-894.